A novel hierarchical fingerprint matching approach ☆

Feng Liu, Qijun Zhao, David Zhang*

Biometrics Research Centre, Department of Computing, The Hong Kong Polytechnic University, Hung Hom, Kowloon, Hong Kong

ARTICLE INFO

ABSTRACT

Fingerprint matching is an important and essential step in automated fingerprint recognition systems (AFRSs). The noise and distortion of captured fingerprints and the inaccurate of extracted features make fingerprint matching a very difficult problem. With the advent of high-resolution fingerprint imaging techniques and the increasing demand for high security, sweat pores have been recently attracting increasing attention in automatic fingerprint recognition. Therefore, this paper takes fingerprint pore matching as an example to show the robustness of our proposed matching method to the errors caused by the fingerprint representation. This method directly matches pores in fingerprints by adopting a coarse-to-fine strategy. In the coarse matching step, a tangent distance and sparse representation-based matching method (denoted as TD-Sparse) is proposed to compare pores in the template and test fingerprint images and establish one-to-many pore correspondences between them. The proposed TD-Sparse method is robust to noise and distortions in fingerprint images. In the fine matching step, false pore correspondences are further excluded by a weighted RANdom SAmple Consensus (WRANSAC) algorithm in which the weights of pore correspondences are determined based on the dis-similarity between the pores in the correspondences. The experimental results on two databases of high-resolution fingerprints demonstrate that the proposed method can achieve much higher recognition accuracy compared with other state-of-the-art pore matching methods.

1. Introduction

Fingerprint matching in automated fingerprint recognition systems (AFRSs) aims to offer a degree of similarity (value between 0 and 1) or a binary decision (matched or non-matched) between two given fingerprint images (template and test fingerprints). Generally, such fingerprints are not compared directly but based on the representation of them, such as minutiae, sweat pore, ridge contour and so on [1], as shown in Fig. 1. Because of noise and distortion introduced during fingerprint capture and the inexact nature of feature extraction, there are errors in the fingerprint representation (e.g. missing, spurious, or noisy features). Therefore, the matching algorithm should be robust to these errors. As the advent of high-resolution fingerprint imaging techniques, new distinctive features, such as sweat pores, ridge contours, ridge edge features, are attracting increasing attention from researchers and practitioners who are working on AFRSs. They also have been proven to be very useful for improving the accuracy of existing minutiae-based AFRSs [2–7]. Sweat pores, among various new features, have attracted the most attention [2–11]. Some effective pore extraction methods have been proposed in [8–12]. However, there are few algorithms for

pore matching [4–7]. The errors mentioned above make fingerprint pore matching very challenging. Thus, this paper takes fingerprint pore matching as an example to introduce our proposed robust fingerprint matching method.

Existing pore matching methods can be roughly divided into two categories. Methods in the first category align the fingerprint images before matching the pores in them [4–6]. Various methods have been proposed for the alignment. Kryszczuk et al. [4] first aligned the test fragmentary fingerprint with the full template fingerprint using the image-correlation-based method, and then matched the pores in the aligned fingerprint images based on their geometric distances. This method has the following two drawbacks: (1) it is time consuming to obtain the best alignment in a quantized transformation parameter space by trying all possible rotations and translations and (2) recognition accuracy heavily relies on the alignment accuracy and is sensitive to the instability of extracted pores and non-linear distortions in fingerprint images. Jain et al. [5,6] proposed a minutiae-based method. The fingerprint images are first aligned by using minutiae. Then, pores lying in a rectangular neighborhood to each aligned minutiae pair are matched using a modified iterative closest point (ICP) algorithm. This method is more efficient than that in [4]. However, it requires a sufficient number of minutiae for effective alignment and considers only the pores in a small neighborhood of aligned minutiae.

Methods in the second category directly match pores in fingerprints without explicit alignment of the fingerprint images. In [7], Zhao et al. proposed a hierarchical coarse-to-fine pore matching
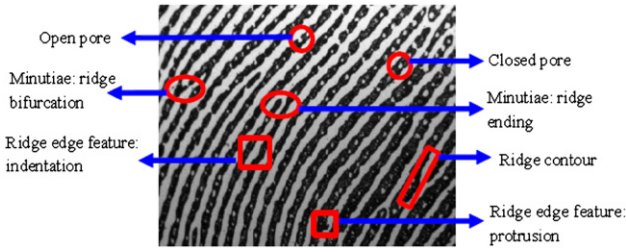
Fig. 1. Features on a high-resolution fingerprint image.

scheme. In the coarse step, one-to-one pore correspondences are roughly determined based on the correlation between the local patches around the pores. In the fine step, the obtained pore correspondences are further refined using a global transformation model. This method has the advantage of robustness to the instability of extracted pores by considering all the available pores in fingerprint images. However, it still has some limitations: (1) the correlation between local patches can be not discriminative enough to ensure that the similarity between a pore and its true corresponding pore is always higher than that between it and the other pores. For example, when the local patches mainly consist of parallel ridges or when they are very noisy or heavily distorted, true pore correspondences could have their similarity ranked not at the top. As a consequence, considering only the top 1 pore correspondences is very likely to miss many true correspondences. (2) Not all the pore correspondences established at the coarse step have the same reliability. Instead, the similarity between the pores in different correspondences can be quite different, and those correspondences with higher similarity are generally believed to be more reliable. Therefore, the similarity of the correspondences provides a natural indicator of their reliability. Yet, previous pore matching methods [7,8] did not explore this information.

In this paper, we propose a novel hierarchical matching method, namely TDSWR, which is less sensitive to the instability of pores and gets rid of the above-mentioned limitations of existing pore matching methods. Compared with existing pore matching methods, the proposed method has the following characteristics: (1) a tangent distance and sparse representation-based matching method (TD-Sparse), which is robust to noise and distortion, is proposed to determine the pore correspondences at the coarse step; (2) one-to-many pore correspondences are established at the coarse step, and thereby most of the true pore correspondences are retained in the results of coarse matching; and (3) a weighted RANdom SAmple Consensus (WRANSAC) algorithm [13], which explores the reliability information of pore correspondences, is employed in the fine matching step to exclude false pore correspondences. Fig. 2 gives the framework of the proposed method.

The rest of this paper is structured as follows. Section 2 introduces the establishment of one-to-many coarse pore correspondences by the TD-Sparse-based matching method. Section 3 presents the WRANSAC algorithm that we have adopted in the fine matching step, and describes in detail the calculation of the weights used in WRANSAC. Section 4 then reports the experiments and analyzes the results. Finally, Section 5 concludes the paper.

2. Coarse pore matching

A key issue in establishing coarse pore correspondences is to calculate the similarities or differences between individual pores. Unlike existing methods [7,8], this paper proposes a TD-Sparse-based method, which is more robust to noise and distortion [18–22], to calculate the differences between pores and establish one-to-many pore correspondences in the coarse pore matching step.
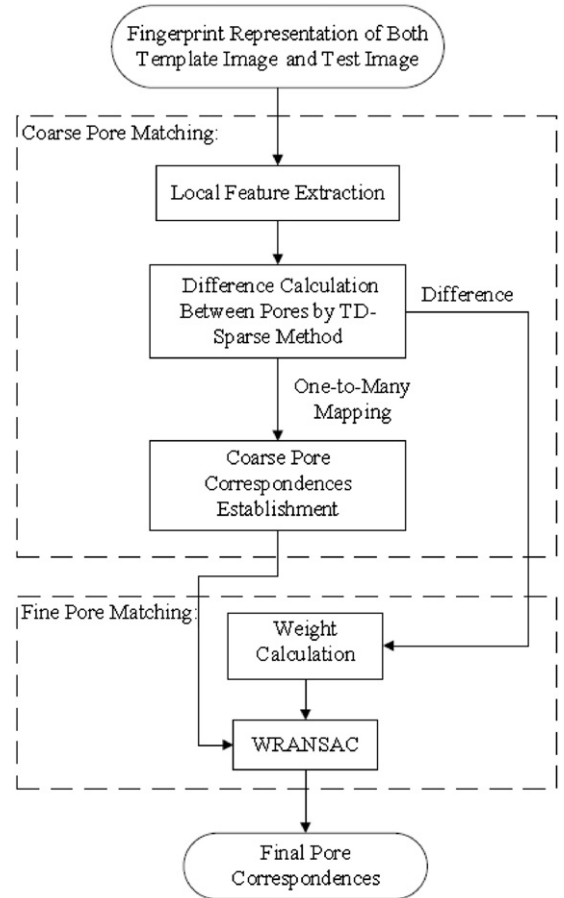

Fig. 2. Framework of the proposed TDSWR method.

A local descriptor is first constructed for each pore. Here, we use the same local descriptor as in [7] so that we can fairly compare the proposed TD-Sparse-based approach and the correlation-based approach in [7]. The local descriptor $p \in \Re^n$ of a pore essentially captures the intensity variation in a circular neighborhood to the pore. To construct the local descriptors, the original fingerprint image is first smoothed by a Gaussian filter. Then, a circular neighborhood to each pore is cropped and rotated to keep the local ridge orientation at the pore horizontal. Finally, the intensity values of the pixels in the neighborhood are concatenated and normalized to form the local descriptor of the pore.

2.1. Difference calculation by TD-Sparse method

To calculate the differences between pores, this paper uses the sparse representation technique rather than the correlation-based technique. Sparse representation was originally developed in signal/image modeling to solve inverse problems [14,15] and began to be practically used with the development of theory and algorithms of l_1-minimization techniques [16,17]. Wright et al. [18] have recently proposed the sparse representation classifier (SRC) for robust face recognition, and obtained promising results. The basic idea of SRC is to represent an input sample by a linear combination of a set of training samples, in which the combination coefficients are restricted to be sparse. It conducts classification based either on the assumption that the coefficients corresponding to the samples of the same class have larger absolute values or on the assumption that the residual of representing the input sample with the samples from the same class is smaller. The procedure of the SRC algorithm is given in Algorithm 1. From the similarity measurement viewpoint,

the coefficient associated with a training sample indicates the similarity between this training sample and the input sample, whereas the residual by each class implies the difference between the input sample and the samples in that class. According to the results in [18], the residuals are more robust to noise than the coefficients. Therefore, in this paper, the differences between pores are measured by the residuals in sparse representation.

Euclidean distance (ED) is used in [18] to calculate the residuals of sparse representation (see Algorithm 1). As a result, the SRC in [18] is sensitive to local distortion, which is however very common in fingerprint images [23]. Therefore, for fingerprint pore matching, we propose to incorporate the tangent distance (TD) into the SRC to make it more robust to distortion.

Algorithm 1. The SRC algorithm [18].

1. **Input**: A set of training samples $A = [A_1, A_2, \ldots, A_k] \in \mathbb{R}^{m \times n}$ of k classes and their class labels, a test sample $y \in \mathbb{R}^m$, as well as an error tolerance $\varepsilon > 0$, or a free parameter $\lambda > 0$ to balance the least squares error of representation and the sparsity of the coefficients.
2. Normalize the columns of A to obtain unit l_2-norm.
3. Solve the l_1-regularized least squares problem (LSP):

$$\hat{x} = \arg\min_x \left\{ \|Ax - y\|_2^2 + \lambda \|x\|_1 \right\} \qquad (1)$$

4. Calculate $\delta_i(x) \in \mathbb{R}^n$, which is a vector whose only nonzero entries are the entries in x that are associated with class i.
5. Compute the residuals: $\delta_i(x)$.
6. **Output**: The category of test sample:

identity$(y) = \arg\min_i r_i(y)$

TD is a distance measure first proposed by Simard et al. [19] for optical character recognition (OCR). It is very effective in handling distortion problems in distance-based classification algorithms. As illustrated in Fig. 3, if ED is used for classification (the Pearson correlation between Fig. 3(a) and (b) (or (c)) is 0.92 (or 0.97) if the ED is used), the fingerprint pattern in Fig. 3(a) will be misclassified into prototype B in Fig. 3(c), but not the true prototype A with slight distortion in Fig. 3(b). On the contrary, TD can easily solve this problem (the Pearson correlation between Fig. 3(a) and (b) (or (c)) is 0.99 (or 0.92) if the TD is used) thanks to its ability to make the input pattern locally invariant to any deformation [19]. In [19], it has also been demonstrated that TD, compared with ED, is closer to the real distance between two patterns in 3-dimensional space.

However, it is difficult to exactly calculate the TD between two patterns. As there is no analytic expression for the manifolds of the patterns, an approximation method has to be adopted. In the following, we provide a procedure [20,21] to calculate the TD between two images, x and y. For the image $x \in \mathbb{R}^{I \times J}$ (I and J represent the numbers of rows and columns, respectively), its corresponding manifold is obtained by applying transforms,

$t(x, \beta)$, to it:

$$M_x = \{t(x, \beta) : \beta \in \mathfrak{R}^C\} \subset \mathfrak{R}^{I \times J} \qquad (2)$$

where $b \in \mathfrak{R}^C$ are the parameters of the transformation, and C is the number of transformation parameters. The approximated manifold is then calculated by Taylor expansion at $\beta = 0$:

$$\hat{M}_x = x + \sum_{k=1}^{C} \beta_k \frac{\partial x}{\partial \beta_k}\bigg|_{\beta_k = 0} + \sum_{k=1}^{C} O(\beta_k^2) \qquad (3)$$

where vector $v_k = (\partial x / \partial \beta_k)|_{\beta_k = 0}$ is called the tangent vector. The TD between images x and y is calculated as follows:

$$\text{TD}(x, y) = \min_{\beta_k} \left\{ \left\| x + \sum_{k=1}^{C} \beta_k v_k - y \right\|_2^2 \right\} \qquad (4)$$

where the tangent vectors $\{v_k\}$ can be either single sided (SD) tangent vectors, i.e. the derivative with respect to x or y, or double sided (DD) tangent vectors, i.e. the derivative with respect to both x and y.

By substituting the ED in the LSP objective function with the above TD, we get the following new objective function of the proposed TD-Sparse method:

$$\hat{x} = \arg\min_x \left\{ \min_{\beta_k} \left\| Ax - \left(y + \sum_{k=1}^{C} \beta_k v_k \right) \right\|_2^2 + \lambda \|x\|_1 \right\} \qquad (5)$$

Although Eq. (5) seems to be a two-step optimization problem, we can solve it as a classical one-step convex optimization problem by combining A and $\{v_k\}$ if single sided tangent vectors from the y side are used here. In this way, Eq. (5) is modified as the following l_1-regularized LSP:

$$\hat{x}' = \arg\min_{x'} \left\{ \|A'x' - y\|_2^2 + \lambda \|x'\|_1 \right\} \qquad (6)$$

Here, $A' = [A \, v_1 \, v_2 \ldots v_L]$, L is the number of tangent vectors. Those tangent vectors $[v_1 \, v_2 \ldots v_L]$ are formed by the differences between y and the transformations of y (rotated, translated or scaled). $x' = [x \, \beta_1 \, \beta_2 \ldots \beta_L]$, and the length of vector x' becomes $n + L$. $[\alpha_1 \, \alpha_2 \ldots \alpha_L]$ are the coefficients of tangent vectors after Taylor expansion. This objective function based on TD can be easily solved by using the same method in solving Eq. (1). Next, we apply the above proposed TD-Sparse method to calculating the difference between pores.

Given input and template fingerprints: S and T, denote the descriptors of the pores in them by $p^S = \{p_1^S, p_2^S, \ldots p_n^S\}$ and $p^T = \{p_1^T, p_2^T, \ldots, p_m^T\}$, where n and m are the number of pores in the input and template fingerprints, respectively. In order to calculate the difference between each pore in S and each pore in T, we take each pore in T as a class, and for each pore in S, we use the linear combination of all the pores in T to approximate it under the sparse representation constraint. According to Eq. (6), the sparse representation coefficients $x_j' = \{x_{j1}', x_{j2}', \ldots, x_{jm}'\}$ for the jth ($j = 1, 2, \ldots, n$) pore

Fig. 3. Examples of fingerprint segments to illustrate the effectiveness of TD compared with ED. (a) A fingerprint pattern that needs to be classified. (b) The prototype A, which is formed by rotating (a) by 10° and then translating it to the left side by 5 pixels. (c) The prototype B, which represents a fingerprint pattern different from (a).

p_j^S in S can be obtained by solving

$$x_j' = \arg\min\left\{\|A'x_j' - p_j^S\|_2^2 + \lambda \sum_{i=1}^{m} |x_{ji}'|\right\} \tag{7}$$

where $A' = [A \; v_1 \; v_2 \ldots v_L]$, A is the basis matrix whose columns are the local descriptors of the pores in T. $x_j' = [x_j \; \alpha_1 \; \alpha_2 \ldots \alpha_L]$. Because non-linear distortions of fingerprints can be locally approximated by linear distortions, we apply the following transformations to p_j^S to generate v_k ($k = 1, 2, \ldots, L$): translation by $[-4:2:4]$ pixels, rotation by $[-9° : 3° : 9°]$ and scaling by $[0.8:0.2:1.2]$. We use the method proposed by Kim et al. [17] to solve Eq. (7). Based on the obtained representation coefficients, we can calculate the difference between the jth ($j = 1, 2, \ldots, n$) pore in S and the ith ($i = 1, 2, \ldots, m$) pore in T as follows:

$$d_{ji} = \left\| p_i^T x_{ji} - p_j^S - \sum_{k=1}^{L} \alpha_k v_k \right\|_2 \tag{8}$$

2.2. Coarse pore correspondence establishment

Coarse pore correspondences are established based on the above calculated differences between pores. Fig. 4 plots the histograms of the differences between 100 pairs of genuine pores (i.e. the same pore in different impressions) and between 100 pairs of imposter pores (i.e. different pores). Obvious overlap can be seen in Fig. 4. This indicates that true pore correspondences can have larger differences than false pore correspondences. Fig. 5 shows two example pores, whose true corresponding pores differ more from them than another two false corresponding pores

because there are mainly parallel ridges in their local neighborhood. Therefore, in order to retain as more true pore correspondences in the coarse matching results as possible, we propose to establish one-to-many coarse pore correspondences as follows.

Given the pair-wise differences between the pores in S and the pores in T, i.e. $\{d_{ji} | j = 1, 2, \ldots, n; \quad i = 1, 2, \ldots, m\}$, the minimum difference between each pore in S and the pores in T is first calculated, denoted as $d_j^{\min} = \min\{d_{ji} | i = 1, 2, \ldots, m\}$ ($j = 1, 2, \ldots, n$). The average of these minimum differences is then computed, i.e. $\bar{d} = (1/n)\Sigma_{j=1}^{n} d_j^{\min}$. Finally, all the pairs of pores whose differences are smaller than $\bar{d}$ compose the set of coarse pore correspondences, i.e.

$$\{(P_l^S, P_q^T) | d_{lq} < \bar{d}\} \tag{9}$$

In this way, one pore can have more than one corresponding pores in the coarse matching results. In other words, one-to-many pore correspondences are established. Fig. 6(a) shows the coarse pore correspondences between two example fingerprint images that are from the same finger.

3. Fine pore matching

Fine pore matching is applied to remove the false pore correspondences in the coarse pore matching results. In [7], a classical RANSAC algorithm is employed. RANSAC [26] outperforms the ICP method, another popularly used method in pore matching [5,6], in its insensitivity to coarse alignment and outliers. It mainly includes two steps which are repeated in an iterative fashion. First, the minimal sample sets (MSSs) are randomly chosen from the dataset,
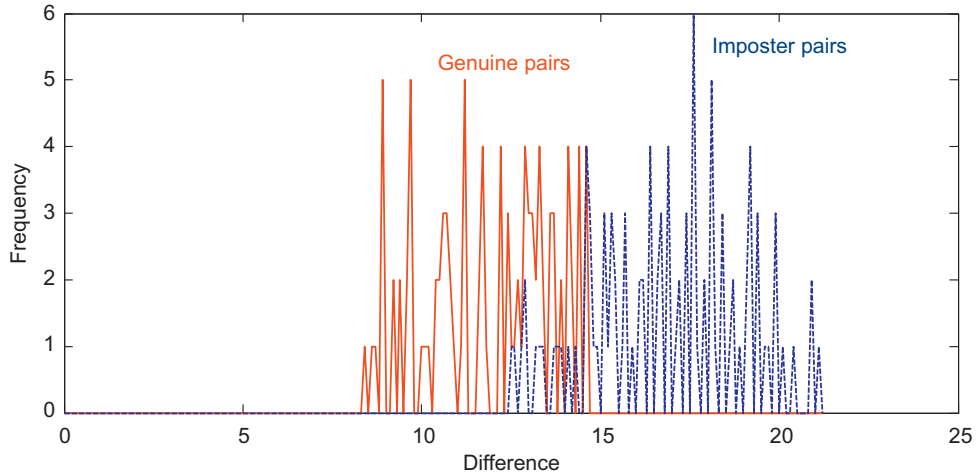

Fig. 4. Histograms of the differences between 100 genuine pore pairs and between 100 imposter pairs.
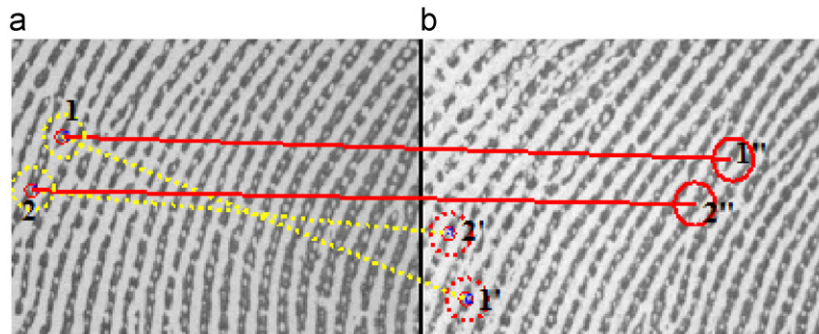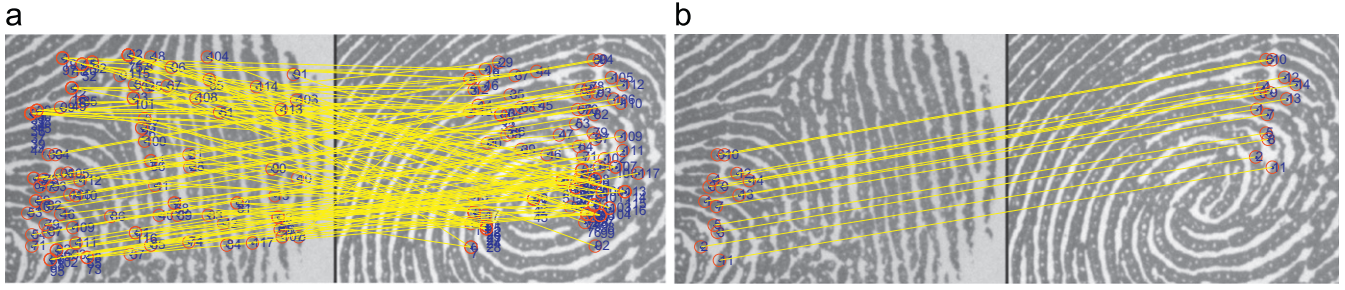

Fig. 5. Two example fingerprint segments from the same finger, which mainly consist of parallel ridges. The differences between the two pores (1 and 2) marked in (a) and their true corresponding pores in (b) (1″ and 2″, marked by solid circles) are larger than the differences between them and another two false corresponding pores in (b) (1′ and 2′, marked by dashed circles).

Fig. 6. Example pore matching results. (a) Coarse pore correspondences in two fingerprint images by the TD-Sparse-based method. (b) Refined pore correspondences in the two fingerprint images by WRANSAC.

and the parameters of the assumed global transformation model are estimated based on MSSs. Second, the other data in the dataset are checked to determine whether they are consistent with the model obtained from the first step. The consistent pairs form the consensus set (CS). RANSAC terminates when the probability of finding a better ranked CS drops below a certain threshold. The selection of MSSs seriously affects the accuracy and efficiency of RANSAC [27]. However, in the classical RANSAC algorithm, all samples in the dataset are chosen with the same probability and without regard to the relative reliability of different samples.

As shown in Fig. 4, even though there are overlaps between the pore differences in genuine and imposter pairs, smaller differences generally indicate that the pore correspondences are more likely resulted from genuine pairs. Therefore, the difference between the pores in a pore correspondence naturally serves as a measure of the reliability of the correspondence. By selecting pore correspondences based on their reliability, we are enabled to more efficiently find true pore correspondences. To implement this, we adopt the Weighted RANSAC (WRANSAC) for fine pore matching. We choose pore correspondences according to the differences between the pores in the correspondences such that the pore correspondences with smaller differences are chosen with a higher probability than those with larger differences. In other words, the pore correspondences with smaller differences are assigned with larger weights. The weights of the pore correspondences are calculated in the following way. Let d_{max} be the maximum difference between all pores on the two fingerprints, i.e. $d_{\max} = \max\{d_{ji}|j=1,2,\ldots,n; i=1,2,\ldots,m\}$. The weight w to the pore correspondence (P_l^S,P_q^T) is then defined by

$$w = 1 - \frac{d_{lq}}{d_{\max}}, \quad d_{lq} < \overline{d} \tag{10}$$

Pore correspondence refinement by WRANSAC proceeds as follows. First, we choose three pairs of corresponding pores to form the MSSs, because we assume that an affine transformation occurs to the fingerprints, and three pore pairs are sufficient to determine the six parameters of an affine model. The MSSs are chosen according to the weights of the pore correspondences. Based on the chosen MSSs, we estimate the six parameters of the affine model by solving a set of linear equations.

Second, we calculate the CS among the coarse pore correspondences under the estimated model parameters. Specifically, the pores in the template fingerprint are transformed according to the obtained model parameters. Then, the distances between them and the pores in the test fingerprint are calculated. The pore pairs whose distances are below a given threshold are taken to be matched. A coarse pore correspondence is taken as an element in the CS if the two pores in the correspondence are still matched after transformation.

The above two steps are repeated until either of the termination conditions is satisfied, and the refined pore correspondences can be obtained once the termination conditions are reached. In this paper, the same two termination conditions as in [7] are used, i.e. the maximum number of iterations N_m (in our experiments, $N_m=1000$) and the sufficient number of iterations N_s. The

sufficient number of iterations is given by

$$N_s = \log(1-p)/\log(1-(1-\varepsilon)^3) \tag{11}$$

where p is the probability that at least one chosen correspondence set MSSs in the iterations is free from false pore correspondences (i.e. outliers), and ε is the percentage of outliers over the entire set of coarse correspondences with respect to the transformation obtained in the current iteration. p is set by experience (in our experiments, $p=0.99$). ε is closely related to the selection of MSSs. Because pore correspondences with smaller differences are more likely to be the correct correspondences, selecting MSSs based on the above defined weights enables a faster selection of the correct MSSs, which then gives a lower percentage of outliers, i.e. a smaller ε. According to Eq. (11), less iteration is then required, i.e. N_s is smaller.

Thanks to the WRANSAC algorithm and the weights we proposed, the above fine pore matching method can find true pore correspondences not only more efficiently, but also more effectively. Fig. 6(b) gives the final pore correspondences obtained from applying WRANSAC to the coarse pore correspondences shown in Fig. 6(a), in which many false pore correspondences are successfully removed. Algorithm 2 summarizes the proposed TDSWR pore matching method.

Algorithm 2. The proposed TDSWR pore matching algorithm.

1. **Input**: Training samples A' consist of the pores in the template fingerprint T and their tangent vectors $[v_1 v_2 \ldots v_L]$, test sample p_i^T from the input fingerprint S, a free parameter $\lambda > 0$ to balance the least squares error of representation and the sparsity of the coefficients.
2. Solve the modified l_1-regularized least squares problem (MLSP):
$$x_j' = \arg\min\left\{\|A'x_j' - p_j^S\|_2^2 + \lambda \sum_{i=1}^m |x_{ji}'|\right\}$$
3. Calculate the difference between the jth ($j=1,2,\ldots,n$) pore in S and the ith ($i=1,2,\ldots,m$) pore in T:
$$d_{ji} = \left\|p_i^T x_{ji} - p_j^S - \sum_{k=1}^L \alpha_k v_k\right\|_2$$
4. Establish coarse pore correspondences:
$$\left\{(P_l^S,P_q^T)|d_{lq} < \overline{d}\right\}$$
$$\overline{d} = \frac{1}{n}\sum_{j=1}^n d_j^{\min}$$
$$d_j^{\min} = \min_i\{d_{ji}|i=1,2,\ldots,m\}, \quad j=1,2,\ldots,n.$$
5. Refine coarse pore correspondences by using WRANSAC algorithm:
   (a) Weight calculation for each coarse pore correspondence:
   $$w = 1 - \frac{d_{lq}}{d_{\max}}, \quad d_{lq} < \overline{d}, \quad d_{\max} = \max\{d_{ji}|j=1,2,\ldots,n; \ i=1,2,\ldots,m\}$$
   (b) Selection of MSSs according to weight.

(c) Model parameter calculation and affine transformation of coarse pore pairs on template fingerprint.

(d) CS establishment.

(e) Final refined pore correspondences once the termination conditions are reached, otherwise, go to step (b).

6. **Output**: Final refined pore correspondences:

$$\{(P_x^S, P_y^T) | x \in l, y \in q\}$$

4. Experimental results and analysis

4.1. Databases

Two databases of high-resolution fingerprint images ($\sim$1200 dpi) were used in the experiments. The first database, denoted as DBI, is the same database as the one used in [7], which contains 1480 fingerprint images from 148 fingers (five images collected for each finger in each of two sessions separated by a time period of about 2 weeks). The images in DBI have a spatial size of 320 pixels $\times$ 240 pixels which covers a small fingerprint area (about 6.5 mm $\times$ 4.9 mm on fingertips). The fingerprint images in the second database (denoted as DBII) were collected in the same way, but with a larger image size, i.e. 640 pixels $\times$ 480 pixels. Pores in these fingerprint images were extracted by using an improved version of the algorithm in [24].

To compare the fingerprint recognition accuracy of the proposed TDSWR method and state-of-the-art methods, including the minutiae- and ICP-based method [5,6] (denoted by MICPP), direct pore matching method [7] (denoted by DP), and classical SRC-based pore matching method (denoted by SRDP) [25], we conducted the following matches for each method on both DBI and DBII. (1) Genuine matches: each of the fingerprint images in the second session was matched with all the fingerprint images of the same finger in the first session, resulting in 3700 genuine match scores. (2) Imposter matches: the first fingerprint image of each finger in the second session was matched with the first fingerprint images of all the other fingers in the first session, resulting in 21,756 imposter match scores. Note that the pore match scores in our experiments were defined as the number of pairs of final matched pores in fingerprints, which was different from the one used in [7]. Based on the obtained match scores, the equal error rates (EER) were calculated for each method.

4.2. Robustness to the instability of extracted pores

In fingerprint pore matching, the instability of pores caused by fingerprint quality (dry or wet) is a crucial issue because it seriously affects the matching results. Fig. 7(a) shows the extracted pores (marked by red dots) in two fingerprint images captured from the same finger at different times. We can see that some pores do not show up, which makes fingerprint pore matching a challenging problem. MICPP only matches the pores that are included in a neighborhood (circled in Fig. 7(a)) to each aligned and matched minutiae pair (connected by lines in Fig. 7(a)). It is thus sensitive to the instability of pores because

the number of reproduced pores in a small region is obviously smaller than that in a large region. On the contrary, TDSWR directly matches pores in a hierarchical way and all of the available pores in the fingerprint images are considered. By applying the MICPP and TDSWR methods to the fingerprints images in Fig. 7(a), 15 and 83 pores are matched, respectively, as shown in Fig. 7(b) and (c). It can be seen that TDSWR is more robust to the instability of pores than MICPP.

Here, it should be noted that the circled neighborhood for MICPP set in this paper is with radius 45. We select such radius by testing different neighborhood radiuses, such as 15, 30, 45, 60, 75, and 90. We found when using small neighborhood (with radius 15 or 30), the number of matched pores is small due to the few number of pore in a small neighborhood. While increasing the radius of neighborhood (45, 60, 75, and 90), more and more false pore correspondences are obtained by MICPP because the local alignment estimated from the mated minutiae cannot be applied to large regions. The middle neighborhood radius 45 is finally chose based on the number of detected matched pore pairs.

4.3. Effectiveness in pore correspondence establishment

Fig. 8 gives the pore correspondences found by different methods in an example genuine pair of fingerprint images in DBI. Fig. 8(a–c) shows the first 20 coarse pore correspondences (red dashed lines denote the false ones) obtained by the correlation-based method, the classical SR-based method, and the TD-Sparse method, respectively. It can be seen that there are 15, 7, and 3 false pore correspondences in the results of the three methods, respectively. Table 1 reports the average number of true pore correspondences among the first 20 coarse pore correspondences (denoted as $\bar{N}_{Top20}$) in 100 pairs of genuine fingerprint images randomly chosen from DBI. These results demonstrate that the proposed TD-Sparse-based method can more accurately determine the coarse pore correspondences than both correlation-based and SR-based methods, because it can better distinguish different pores and is more robust to noise and non-linear distortion, which are very common in fingerprint images.

Fig. 8(d) and (e) shows the final pore correspondences by applying the classical RANSAC and the WRANSAC to the coarse pore correspondences established by the TD-Sparse method. WRANSAC found 41 pore correspondences, whereas RANSAC found only 27 pore correspondences. Obviously, WRANSAC is more effective in refining pore correspondences. Moreover, according to our experimental results on DBI, on average, WRANSAC converges in 174 iterations, whereas RANSAC converges in 312 iterations. Hence, WRANSAC is also more efficient than RANSAC.

4.4. Fingerprint recognition performance

In order to illustrate the importance of one-to-many coarse pore correspondences for accurate fingerprint recognition, we compare the EERs on DBI by using one-to-many TD-Sparse (denoted as 1toM_TD-Sparse), one-to-one TD-Sparse (denoted as 1to1_TD-Sparse) and one-to-one correlation-based (denoted as
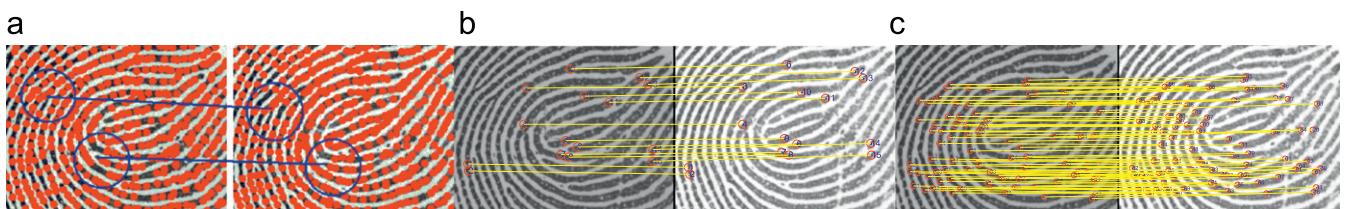
Fig. 7. Example pore matching results of MICPP and TDSWR. (a) Two example fingerprint images with extracted pores and corresponding minutiae. (b) Final pore correspondences obtained by MICPP. (c) Final pore correspondences obtained by TDSWR.
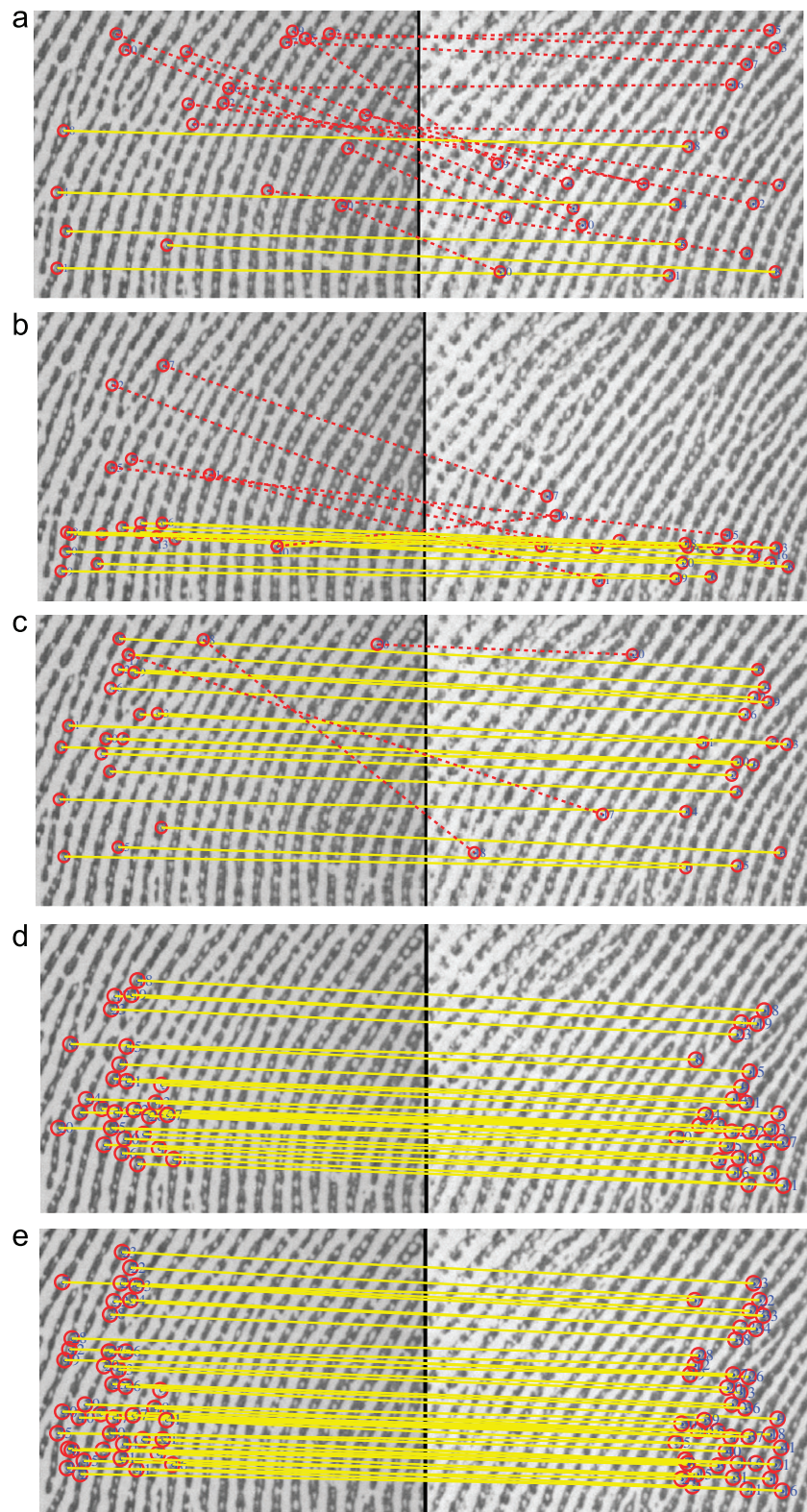
Fig. 8. Example pore correspondence establishment results. The first 20 coarse pore correspondences obtained by (a) correlation, (b) SR, and (c) TD-Sparse-based methods. Final pore correspondences obtained by applying (d) RANSAC and (e) WRANSAC to the coarse pore correspondences established by the TD-Sparse method.

1to1_Correlation) methods to establish coarse pore correspondences and using RANSAC to refine the pore correspondences. Here, we choose RANSAC algorithm because there are no weights available for 1to1_Correlation method in [7]. The results are presented in Table 2. As can be seen, the lowest EER is obtained

by 1toM_TD-Sparse, which shows the effectiveness of one-to-many coarse pore correspondences in improving fingerprint recognition accuracy.

We finally compare the fingerprint recognition performance of the proposed TDSWR method, the MICPP, DP, and SRDP methods

on DBI and DBII. Fig. 9 shows the ROC curves of these methods, and the corresponding EERs are listed in Table 3. It can be seen that TDSWR outperforms both MICPP and DP by decreasing the EER by one order of magnitude on both DBI and DBII. Compared with SRDP, TDSWR has also improved the EER by more than 50% and 45% on DBI and DBII, respectively. This fully demonstrates the effectiveness of TD over ED for fingerprint pore matching.

We believe that the improvement achieved by the proposed TDSWR method owes to the following three factors. First, the hierarchical strategy makes the matching method more robust to the instability of pores. Second, the TD-Sparse method used to find coarse pore correspondences is not only robust to noise, which has been demonstrated in [18], but also robust to fingerprint distortion by using TD instead of ED in sparse representation. Third, the one-to-many coarse pore correspondence establishment scheme together with the WRANSAC-based refinement make it more effective and efficient to find the correct pore correspondences in fingerprints.

4.5. TDSWR applied in fingerprint minutiae matching

The proposed TDSWR is also suitable for minutiae matching in fingerprints. Fig. 10 shows an example of fingerprint matching results based on minutiae. From the extracted result in Fig. 10(a), we can see

Table 1
Average number of true pore correspondences among the first 20 coarse pore correspondences ($\overline{N}_{Top20}$) in 100 genuine fingerprint pairs randomly selected from DBI.

Method	$\overline{N}_{Top20}$
Correlation-based method	8
SR-based method	11
TD-Sparse-based method	14

Table 2
EER of pore matching with different coarse pore correspondence establishment methods.

Database EER (%) method	DBI
1to1_Correlation	15.42
1to1_TD-Sparse	5.82
1toM_TD-Sparse	4.45

that there are missing (solid circled), spurious (dashed circled), and inaccurate extracted (solid rectangled) minutiae in both compared fingerprints. Our proposed method can effectively establish the coarse correspondences, as shown in Fig. 10(b); there are 5 wrong correspondences in 24 coarse ones. 15 true correspondences are finally selected out after refinement, as shown in Fig. 10(c). Fig. 11 also shows the fingerprint recognition performance (ROC) of minutiae-based matching in DBII by using the proposed TDSWR method. The EER is about 11%, which further demonstrates the effectiveness of our proposed method for fingerprint matching.

This example matching also demonstrates that our proposed TDSWR method can be used for other image matching problems. It is because this approach firstly constructs a local descriptor at the location of each feature point, and then establishes coarse correspondences and refines the coarse pairs to get final result. The proposed TD-Sparse and WRANSAC methods are useful for any coarse matching and fine matching. Therefore, this method can be modified to solve different image matching problems by constructing different local descriptor or using different coarse (or fine) matching methods.

5. Conclusions and future work

This paper has proposed a novel hierarchical fingerprint matching method, namely TDSWR, which was mainly applied in sweat pore, by introducing the TD-Sparse-based method for coarse pore correspondence establishment and WRANSAC for refinement. The proposed method measures the differences between pores based on the residuals obtained by tangent distance and sparse representation technique, which makes our method more robust to noise and local distortions in fingerprints when compared with the existing DP and SRDP method. It then establishes one-to-many coarse pore correspondences, and assigns to each correspondence a weight-based on the difference between the pores in the correspondence. The final pore correspondences are obtained by adopting
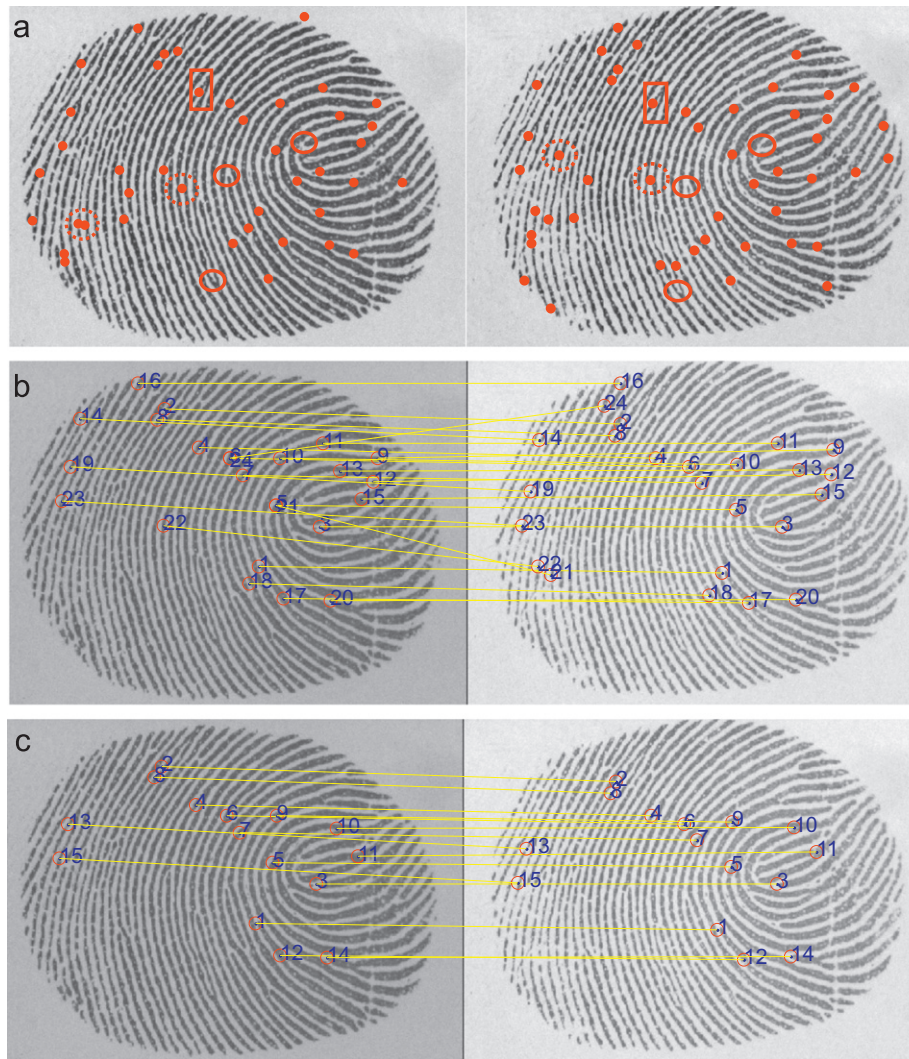
Table 3
EER of different pore matching methods.

| Database EER (%) method	DBI	DBII
MICPP	30.45	7.83
DP	15.42	7.05
SRDP	6.59	0.97
TDSWR	3.25	0.53
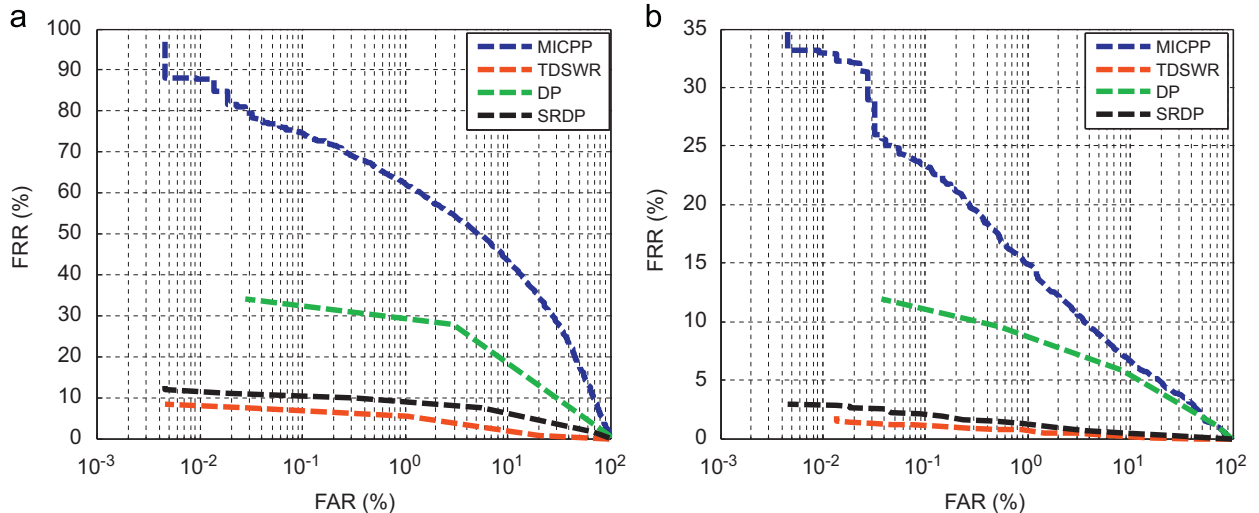
Fig. 9. ROCs of different pore matching methods on (a) DBI and (b) DBII.

Fig. 10. Example matching results of TDSWR based on minutiae. (a) Two example fingerprint images with dotted extracted minutiae (41 in the left print and 47 in the right print). (b) Coarse minutiae correspondences (24 initial obtained minutiae pairs). (c) Final minutiae correspondences (15 true minutiae pairs).
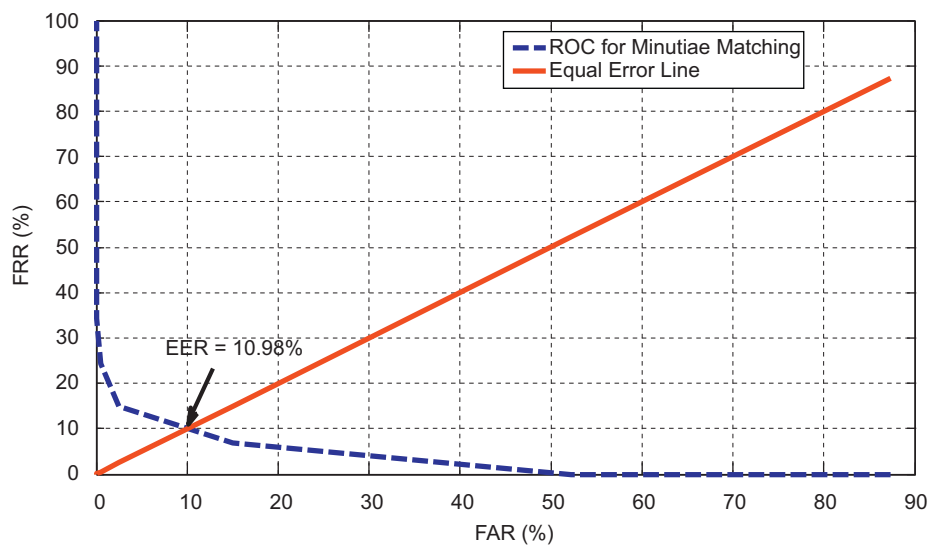
Fig. 11. ROC for minutiae-based matching using TDSWR in DBII.

WRANSAC to refine coarse pore correspondences. The experimental results demonstrate that the proposed method can more effectively establish pore correspondences and finally reduce the EER by one order of magnitude in both of the two fingerprint databases used in the experiments (the best improvement on the recognition accuracy is up to 92%). However, the high computational complexity is one of

the limitations of the proposed method. How to further improve the efficiency of the proposed pore matching method is among our future work. One possible solution is first aligning two fingerprints to estimate the overlapping area between them and then matching only the pores lying in the overlapping area.

It is more valuable that the method proposed in this paper can be used for any other image matching problems if slightly modified or not. For example, it can be directly used for singular point and minutiae matching in fingerprints. By constructing different local descriptor or using different coarse (or fine) matching methods, this method is also effective to solve different image matching problems.

Acknowledgements

References

[1] CDEFFS, Data format for the interchange of extended fingerprint and palmprint features, Working Draft Version 0.4, ⟨http://fingerprint.nist.gov/standard/cdeffs/index.html⟩, June 2009.

[2] J.D. Stosz, L.A. Alyea, Automated system for fingerprint authentication using pores and ridge structure, in Proceedings of SPIE Conference on Automatic Systems for the Identification and Inspection of Humans, San Diego, 1994, pp. 210–223.

[3] A. Roddy, J. Stosz, Fingerprint features—statistical analysis and system performance estimates, Proceedings of the IEEE 85 (9) (1997) 1390–1421.

[4] K. Kryszczuk, P. Morier, A. Drygajlo, Study of the distinctiveness of level 2 and level 3 features in fragmentary fingerprint comparison, in: Proceedings of the BioAW2004, LNCS, 2004, pp. 124–133.

[5] A. Jain, Y. Chen, M. Demirkus, Pores and ridges: fingerprint matching using level 3 features, in: Proceedings of the18th International Conference on Pattern Recognition, vol. 4, 2006, pp. 477–480.

[6] A.K. Jain, Y. Chen, M. Demirkus, Pores and ridges: high-resolution fingerprint matching using level 3 features, IEEE Transactions on Pattern Analysis and Machine Intelligence 29 (1) (2007) 15–27.

[7] Q. Zhao, L. Zhang, D. Zhang, N. Luo, Direct pore matching for fingerprint recognition, in: Proceedings of ICB'09, 2009, pp. 97–606.

[8] Q. Zhao, High Resolution Fingerprint Additional Features Analysis, The Hongkong Polytechnic Univeristy, 2010.

[9] K. Kryszczuk, A. Drygajlo, P. Morier, Extraction of level 2 and level 3 features for fragmentary fingerprints, in: Proceedings of the Second COST Action 275 Workshop, Vigo, Spain, 2004, pp. 83–88.

[10] M. Ray, P. Meenen, R. Adhami, A novel approach to fingerprint pore extraction, in: Proceedings of the 37th South-eastern Symposium on System Theory, 2005, pp. 282–286.

[11] N.R. Parsons, J.Q. Smith, E. Thonnes, L. Wang, R.G. Wilson, Rotationally invariant statistics for examining the evidence from the pores in fingerprints, Law, Probability and Risk 7 (2008) 1–14.

[12] Q. Zhao, D. Zhang, L. Zhang, N. Luo, Adaptive fingerprint pore modeling and extraction, Pattern Recognition 43 (8) (2010) 2833–2844.

[13] D. Zhang, W. Wang, Q. Huang, S. Jiang, W. Gao, Matching images more efficiently with local descriptors, in: Proceedings of the 19th International Conference on Pattern Recognition, 2008.

[14] D. Donoho, For most large underdetermined systems of linear equations the minimal l_1-norm solution is also the sparsest solution, Communications on Pure and Applied Mathematics 59 (6) (2006) 797–829.

[15] I. Daubechies, M. Defriese, C. DeMol, An iterative thresholding algorithm for linear inverse problems with a sparsity constraint, Communications on Pure and Applied Mathematics 57 (11) (2004) 1413–1457.

[16] S. Boyd, L. Vandenberghe, Convex Optimization, Cambridge University, 2004.

[17] S.J. Kim, K. Koh, M. Lustig, S. Boyd, D. Gorinevsky, A method for large-scale l_1-regularized least squares, IEEE Journal on Selected Topics in Signal Processing 1 (4) (2007) 606–617.

[18] J. Wright, A. Yang, A. Ganesh, S. Sastry, Y. Ma, Robust face recognition via sparse representation, IEEE Transactions on Pattern Analysis and Machine Intelligence 31 (2) (2009) 210–227.

[19] P. Simard, Y. Cun, and J. Denker, Efficient pattern recognition using a new transformation distance, in: Proceedings of Advances in Neural Information Processing Systems 5 (NIPS Conference), 1992, pp. 50–58.

[20] D. Keysers, J. Dahmen, T. Theiner, H. Ney, Experiments with an extended tangent distance, in: Proceedings of the 15th International Conference on Pattern Recognition, 2000, pp. 2038–2041.

[21] D. Keysers, W. Macherey, H. Ney, J. Dahmen, Adaptation in statistical pattern recognition using tangent vectors, IEEE Transactions on Pattern Analysis and Machine Intelligence 26 (2) (2004) 269–274.

[22] S. Yan, H. Wang, Semi-supervised learning by sparse representation, in: Proceedings of SIAM International Conference on Data Mining, 2009, pp. 792–801.

[23] A. Ross, S. Dass, A. Jain, A deformable model for fingerprint matching, Pattern Recognition 38 (1) (2005) 95–103.

[24] Q. Zhao, L. Zhang, D. Zhang, N. Luo, J. Bao, Adaptive pore model for fingerprint pore extraction, in: Proceedings of the 19th International Conference on Pattern Recognition, 2008, pp. 1–4.

[25] F. Liu, Q. Zhao, L. Zhang, D. Zhang, Fingerprint pore matching based on sparse representation, in: Proceedings of the 20th International Conference on Pattern Recognition, 2010.

[26] M. Fishler, R. Bolles, Random sample consensus: a paradigm for model fitting with applications to image analysis and automated cartography, Communications of the ACM 24 (6) (1981) 381–395.

[27] M. Zuliani, RANSAC for Dummies, MathWorks, ⟨http://www.mathworks.com⟩, November 2008.

Feng Liu received her B.S. and M.S. degrees both from the Department of Electrical and Engineering, Xidian University, Xi'an, Shaanxi, China, respectively, in 2006 and 2009. She is now a Ph.D. student in computer science of the Department of Computing at the Hong Kong Polytechnic University. Her research interests include pattern recognition and image processing, especially focus on their applications to fingerprints.

David Zhang graduated in Computer Science from Peking University. He received his M.Sc. in Computer Science in 1982 and his Ph.D. in 1985 from the Harbin Institute of Technology (HIT). From 1986 to 1988 he was a Postdoctoral Fellow at Tsinghua University and then an Associate Professor at the Academia Sinica, Beijing. In 1994 he received his second Ph.D. in Electrical and Computer Engineering from the University of Waterloo, Ontario, Canada. Currently, he is a Head, Department of Computing, and a Chair Professor at the Hong Kong Polytechnic University where he is the Founding Director of the Biometrics Technology Centre (UGC/CRC) supported by the Hong Kong SAR Government in 1998. He also serves as Visiting Chair Professor in Tsinghua University, and Adjunct Professor in Shanghai Jiao Tong University, Peking University, Harbin Institute of Technology, and the University of Waterloo. He is the Founder and Editor-in-Chief, International Journal of Image and Graphics (IJIG); Book Editor, Springer International Series on Biometrics (KISB); Organizer, the first International Conference on Biometrics Authentication (ICBA); Associate Editor of more than ten international journals including IEEE Transactions and Pattern Recognition; Technical Committee Chair of IEEE CIS and the author of more than 10 books and 200 journal papers. Professor Zhang is a Croucher Senior Research Fellow, Distinguished Speaker of the IEEE Computer Society, and a Fellow of both IEEE and IAPR.

Qijun Zhao received his B.S. and M.S. degrees both from the Department of Computer Science and Engineering, Shanghai Jiao Tong University, Shanghai, China. He was a Ph.D. student at the Department of Computing, Hong Kong Polytechnic University when the work in this paper was conducted. In 2010, he got his Ph.D. degree from there and is now working as a Post-Doctoral fellow at the Pattern Recognition and Image Processing Lab, Michigan State University, East Lansing, MI, United States. His research interests mainly lie in the fields of pattern recognition, machine learning, image processing, and artificial intelligence, with applications to biometrics, information security, and intelligent systems.